

RESEARCH

Open Access



# Risk analysis of grade $\geq 2$ radiation pneumonitis based on radiotherapy timeline in stage III/IV non-small cell lung cancer treated with volumetric modulated arc therapy: a retrospective study

Songhua Yang<sup>1†</sup>, Shixiong Huang<sup>2†</sup>, Xu Ye<sup>2</sup>, Kun Xiong<sup>3</sup>, Biao Zeng<sup>2</sup> and Yingrui Shi<sup>2\*</sup>

## Abstract

**Background:** Radiotherapy is an important treatment for patients with stage III/IV non-small cell lung cancer (NSCLC), and due to its high incidence of radiation pneumonitis, it is essential to identify high-risk people as early as possible. The present work investigates the value of the application of different phase data throughout the radiotherapy process in analyzing risk of grade  $\geq 2$  radiation pneumonitis in stage III/IV NSCLC. Furthermore, the phase data fusion was gradually performed with the radiotherapy timeline to develop a risk assessment model.

**Methods:** This study retrospectively collected data from 91 stage III/IV NSCLC cases treated with Volumetric modulated arc therapy (VMAT). Patient data were collected according to the radiotherapy timeline for four phases: clinical characteristics, radiomics features, radiation dosimetry parameters, and hematological indexes during treatment. Risk assessment models for single-phase and stepwise fusion phases were established according to logistic regression. In addition, a nomogram of the final fusion phase model and risk classification system was generated. Receiver operating characteristic (ROC), decision curve, and calibration curve analysis were conducted to internally validate the nomogram to analyze its discrimination.

**Results:** Smoking status, PTV and lung radiomics feature, lung and esophageal dosimetry parameters, and platelets at the third week of radiotherapy were independent risk factors for the four single-phase models. The ROC result analysis of the risk assessment models created by stepwise phase fusion were: (area under curve [AUC]: 0.67, 95% confidence interval [CI]: 0.52–0.81), (AUC: 0.82, 95%CI: 0.70–0.94), (AUC: 0.90, 95%CI: 0.80–1.00), and (AUC: 0.90, 95%CI: 0.80–1.00), respectively. The nomogram based on the final fusion phase model was validated using calibration curve analysis and decision curve analysis, demonstrating good consistency and clinical utility. The nomogram-based risk

<sup>†</sup>Songhua Yang and Shixiong Huang contributed equally to this work and should be considered co-first authors.

\*Correspondence: shiyingrui@hnca.org.cn

<sup>2</sup> Department of Radiation Oncology, Hunan Cancer Hospital/the Affiliated Cancer Hospital of Xiangya School of Medicine, Central South University, Changsha 410013, Hunan, People's Republic of China

Full list of author information is available at the end of the article



classification system could correctly classify cases into three diverse risk groups: low-(ratio:3.6%;  $0 < \text{score} < 135$ ), intermediate-(ratio:30.7%,  $135 < \text{score} < 160$ ) and high-risk group (ratio:80.0%,  $\text{score} > 160$ ).

**Conclusions:** In our study, the risk assessment model makes it easy for physicians to assess the risk of grade  $\geq 2$  radiation pneumonitis at various phases in the radiotherapy process, and the risk classification system and nomogram identify the patient's risk level after completion of radiation therapy.

**Keywords:** Radiation pneumonitis, Radiotherapy timeline, Nomogram, Risk classification system

## Background

Non-small-cell lung cancer (NSCLC) accounts for 85% of all lung cancer cases [1]. Many NSCLC cases were diagnosed as stage III/IV and lost the opportunity for surgery, making it a major cause of cancer-associated death globally [2]. Therefore, systemic therapy was the main therapeutic modality for stage III/IV NSCLC, with radiotherapy playing an important role. Radiation pneumonitis (RP) was the most common and potentially devastating side effect of thoracic radiotherapy, occurring within 6 months post-RT. It caused chronic respiratory insufficiency, even severely affect patients' life quality, caused the dismal prognostic outcome, and even death [3–5]. Patients with III/IV NSCLC have the highest risk of RP, with data from studies reporting up to 30 to 40% [6]. Therefore, it is essential among III/IV NSCLC cases to identify toxicity in RT as soon as possible. Moreover, it is necessary to accurately assess the RP risk, allowing for personalized RT dosing and maximized therapeutic benefits.

Numerous studies have been conducted to investigate clinical risk factors for RP, such as pulmonary function, performance status, smoking history, tumor location, an interstitial pulmonary disorder, pulmonary emphysema, and concurrent chemotherapy, all of which are strongly associated with the occurrence of RP [6–11]. Previously, RP has been reported to be related to dosimetric factors derived from dose-volume histograms, such as average lung dose, V5, V20, or dosimetric parameters [12–15]. As radiomics analytical techniques rapidly develop, research on RT therapeutic benefits and estimating its adverse reactions according to radiomics characteristics have become the research hotspots [16–19]. As per an article, changes in certain radiomics characteristics were dose-dependently related to RP grade  $\geq 2$  determined by obtaining local lung CT images post-RT [18]. In addition, a study constructed the model to differentiate patients with high-risk RP from low-risk RP by analyzing the region of interest (ROI) within the entire lung tissue prior to RT [19]. Briefly, radiomics characteristics can be used to obtain lung texture characteristics and aid in describing possible RP risk [20, 21]. However, the vast majority of studies and analyses were based on one individual data type or a simple combination of several data types.

In practice, the duration of the radiotherapy process can take up to 8–10 weeks and consists of four phases: admission examination, target delineation, plan design, and radiotherapy implementation. Different types of data can be available at different radiotherapy phases; therefore, a longitudinal analysis of radiotherapy data based on a timeline may be more meaningful.

The present work investigated the potential risk factors for RP at different phases of radiotherapy for stage III/IV NSCLC, then fused the data of different phases based on the radiotherapy timeline to improve the effectiveness of the model, and finally established the risk classification system and nomogram according to fusion model of all phases data. In the age of precision radiotherapy, these tools can help physicians identify patients with RP as early as possible, allowing them to customize follow-up treatment strategies and interventions.

## Materials and methods

### Patient cohort

The present retrospective study included 91 cases between June 2019 and June 2021. All patients were diagnosed with stage III/IV NSCLC according to the AJCC 8th edition. Inclusion criteria: (1) No contraindication to RT and estimated survival greater than 6 months after RT. (2) No intolerance or interruption of RT for more than a week. (3) Absence of acute infectious or autoimmune disease. (4) Complete follow-up information. The gross tumor volume (GTV), planning target volume (PTV), and clinical target volume (CTV) as defined in ICRU 50 and 62 were measured in this study. Furthermore, this study described risky organs and target volumes based on RT and oncologic group guidelines. The prescribed RT doses were 50–66 Gy at 1.8–2 Gy/fraction/day for five fractions/week. Each RT plan was obtained from the Eclipse system (Varian Medical Systems, Palo Alto, CA, version 13.5.35), which was delivered with 6 MV photon beams and 2-arc VMAT. Patients were given either simultaneous chemoradiation or sequential chemoradiation. The chemotherapy regimens contained Carboplatin-based doublet, Cisplatin-based doublet, Platinum-based triplet, Single agent and Other which were applied in a widespread manner in clinical settings. Doses and regimens were modified according to

the National Comprehensive Cancer Network (NCCN) and the Chinese Society of Clinical Oncology (CSCO). Informed consent was not required as this is a retrospective, unicentric cohort study.

**Evaluation of RP**

All cases were assessed every week during the process of RT. Follow-up visits were made 1 month after RT and every 2–3 months for the next 6 months. RP was graded by one senior radiologist and two senior oncologists. RP severity was assessed by the National Cancer Institute Common Terminology Criteria for Adverse Events 4.03 (CTCAE 4.03). A grade  $\geq 2$  was considered symptomatic RP, which required steroids or limiting instrumental activities of daily living. Therefore, the endpoint was Grade  $\geq 2$  RP (RP  $\geq 2$ ) in our study.

**Four-phase characterization based on radiotherapy timeline**

This study was used to investigate RP  $\geq 2$  risk by collecting data at four different phases, as shown in Fig. 1 (1) General clinical characteristics of patients at the admission examination phase (Phase I): age, BMI, sex, ECOG score, smoking status, diabetes, hypertension, emphysema, chronic obstructive pulmonary disease (COPD), Clinical stages, surgical history, and chemoradiation. (2) Radiomics feature at target area delineation phase (Phase II): Radiomics feature of PTV and lungs. (3) radiation dosimetry parameters during the RT plan design phase (Phase III): lungs Vx-V50 (by 5), mean lung dose, Heart V5-V50 (by 10), mean heart dose, esophagus V5-V50 (by

10), mean esophagus dose, and maximum spinal cord dose. This study defined lung as (left+right lung)-GTV, whereas Vx as total lung volume that received xGy or higher level of radiation. (4) Hematological indexes of patients during the radiotherapy implementation phase (Phase IV): This study required neutrophils, lymphocytes, monocytes, erythrocytes, hemoglobin, and platelets at three distinct time intervals with 1 week before RT (baseline), 3 weeks (3w) during RT, and 5 weeks (5w) during RT.

**CT image acquisition and radiomics features extraction**

All cases were subjected to free-breathing CT scans using a Philips Brilliance Big Bore CT scanner (Philips Medical Systems, Inc., Cleveland, OH) to develop treatment plans. The following parameters were used in CT scans: tube current (200mA), voltage (120 kVp), pixel size (0.911 mm), slice thickness (5 mm), and image matrices (X: 768, Y: 768). This work utilized the Pyradiomics library in Python for extracting radiomic features. One hundred five Original features were extracted, including 18 first-order features, 14 shape features, and 73 texture analysis features (Gray Level Concurrence/Run Length/Size Zone/Dependence Matrix [GLCM/GLRLM/GLSZM/GLDM features, Neighborhood gray-tone difference matrix [NGTDM] features) were extracted. A total of 1183 transformation features based on shape and first order were extracted. Eight wavelet filters (LHL, HLL, LLH, LHH, HHH, HLH, LLL, and HHL) and five Image algorithms (square root, square, gradient, exponential, logarithm) were used. Prior to calculating

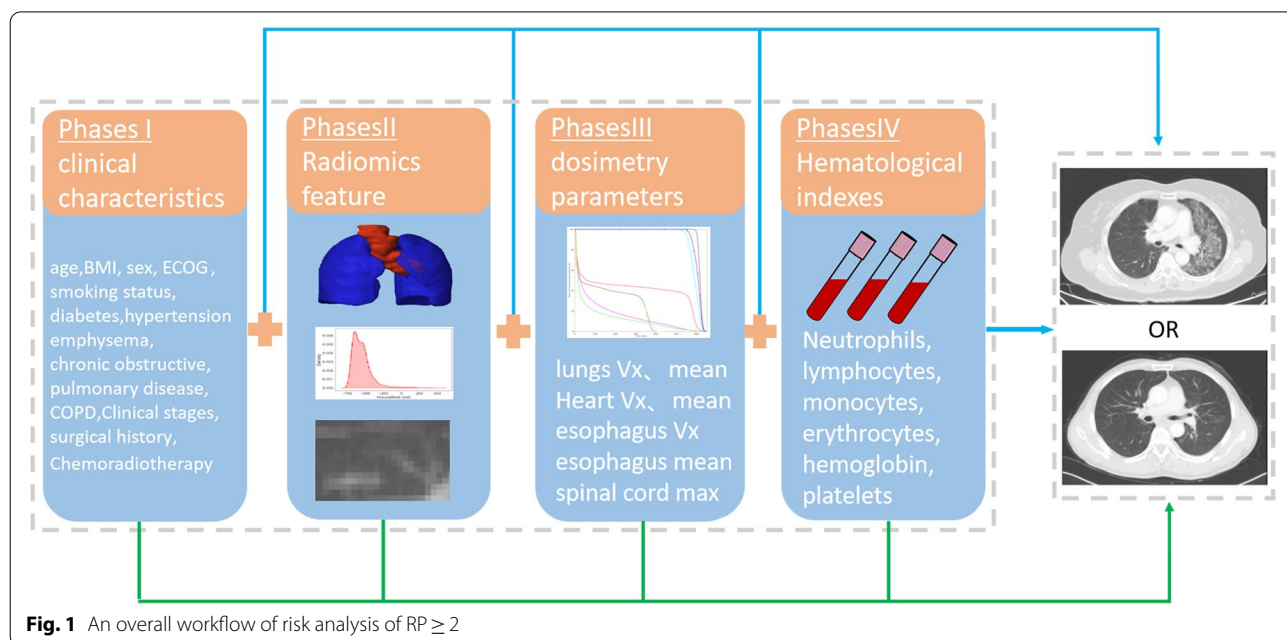


**Fig. 1** An overall workflow of risk analysis of RP  $\geq 2$

radiomics features, each image was resampled (size:  $3 \times 3 \times 3$ ) and normalized (normalize Scale:100). We obtained 2576 features in PTV and lungs by performing the above operations.

**Statistical analysis**

Univariate analysis was performed on Phase I/III/IV data. T-test and chi-square tests were used to calculate *P*-values for continuous and categorical variables, respectively. Subsequently, parameters of *P* < 0.05 were selected for multivariate analysis. This work utilized the least absolute shrinkage and selection operator (LASSO) algorithm for Phase II data for the sake of selecting significant features. Meanwhile, this work reduced coefficients of the unrelated radiomics feature to 0, while those (non-0) of the rest features closely associated with  $RP \geq 2$  were selected for multivariate analysis. The four Phases (I/II/III/IV) data were analyzed by multivariate analysis to establish the risk analysis model, and the significant risk factors of a single-phase model were included in the fusion phases (I~II/I~III/I~IV) model. The stepwise logistic regression was utilized in multivariate analysis. This work determined Spearman’s correlation coefficients in all models, with a result greater than 0.8 indicating potent correlation. For two closely related features, the feature with an larger univariate analysis *p*-value was removed [22, 23]. Variance Inflation Factor (VIF) is used to detect the presence of multicollinearity in model features. This work also plotted receiver operating characteristic (ROC) curves for evaluating model classification performance. Python and R software (version 3.5.3) was used for data analysis and visualization.

**Nomogram and risk classification system establishment and verification**

This study developed a visual nomogram based on the fusion model of all phases data. As revealed by calibration curves (resampling of 1000 bootstraps), for  $RP \geq 2$ , the nomogram-predicted probability was consistent with the actual value. Moreover, this work utilized the decision curve analysis (DCA) for testing nomogram utility in the clinic. The total risk point was assessed using our nomogram; then, recursive partitioning analysis was performed to develop the risk classification system for the accurate and effective classification of cases in diverse  $RP \geq 2$  risk levels.

**Results**

**Univariate regression and radiomics feature selection**

The general clinical characteristics (Phase I) are shown in Table 1. In general, the incidence of  $RP \geq 2$  is 19.8% (18/91), of which sex (*P* = 0.01), BMI (*P* = 0.03), and smoking status (*P* = 0.004) showed significant

**Table 1** Univariate analysis results of clinical characteristics in Phases I

Clinical characteristics	RP < 2 (n = 73)	RP ≥ 2 (n = 18)	p-value
Age (year)	58.9 (8.8)	60.0 (6.5)	0.619
BMI	23.0 (2.5)	24.6 (2.8)	0.030*
Sex			0.010*
male	61 (85.92%)	10 (14.08%)	
female	12 (60.0%)	8 (40.0%)	
ECOG			0.279
0	19 (73.08%)	7 (26.92%)	
1	54 (83.08%)	11 (16.92%)	
Smoking Status			0.004**
yes	57 (87.69%)	8 (12.31%)	
No	16 (61.54%)	10 (38.46%)	
Diabetes			0.588
yes	7 (87.5%)	1 (12.5%)	
no	66 (79.52%)	17 (20.48%)	
Hypertension			0.342
yes	13 (72.22%)	5 (27.78%)	
no	60 (82.19%)	13 (17.81%)	
Emphysema			0.285
yes	11 (91.67%)	1 (8.33%)	
No	62 (78.48%)	17 (21.52%)	
COPD			0.704
yes	6 (85.71%)	1 (14.29%)	
no	67 (79.76%)	17 (20.24%)	
Clinical Stages			0.704
III	67 (79.76%)	17 (20.24%)	
IV	6 (85.71%)	1 (14.29%)	
Surgical History			0.666
yes	13 (76.47%)	4 (23.53%)	
no	60 (81.08%)	14 (18.92%)	
Chemoradiotherapy			0.871
concurrent	34 (80.95%)	8 (19.05%)	
sequential	39 (79.59%)	10 (20.41%)	

1. Data are Mean (standard deviation) or number of patients (percentages);  
 2.\**P* < 0.05, \*\**P* < 0.01

differences of  $RP \geq 2$  when compared with  $RP < 2$  groups. Lasso regression of Radiomics features (Phase II) is shown in Fig. 2. The feature selection results, which included PTV (2 shapes, 1 texture) and lung (5 first-order, 2 textures), are represented in Table 2. Radiation dosimetry parameters (Phase III) are shown in Table 3, where lungs v5–20 (by 5) and esophagus v10–20 (by 10) are significantly different (*P* < 0.05) between the  $RP \geq 2$  group and  $RP < 2$  group. Hematological indexes (Phase IV) are shown in Table 4. With the increase of RT weeks, the values of lymphocytes, erythrocytes, hemoglobin, and platelets show a decreasing trend. Among them, platelet in the third week

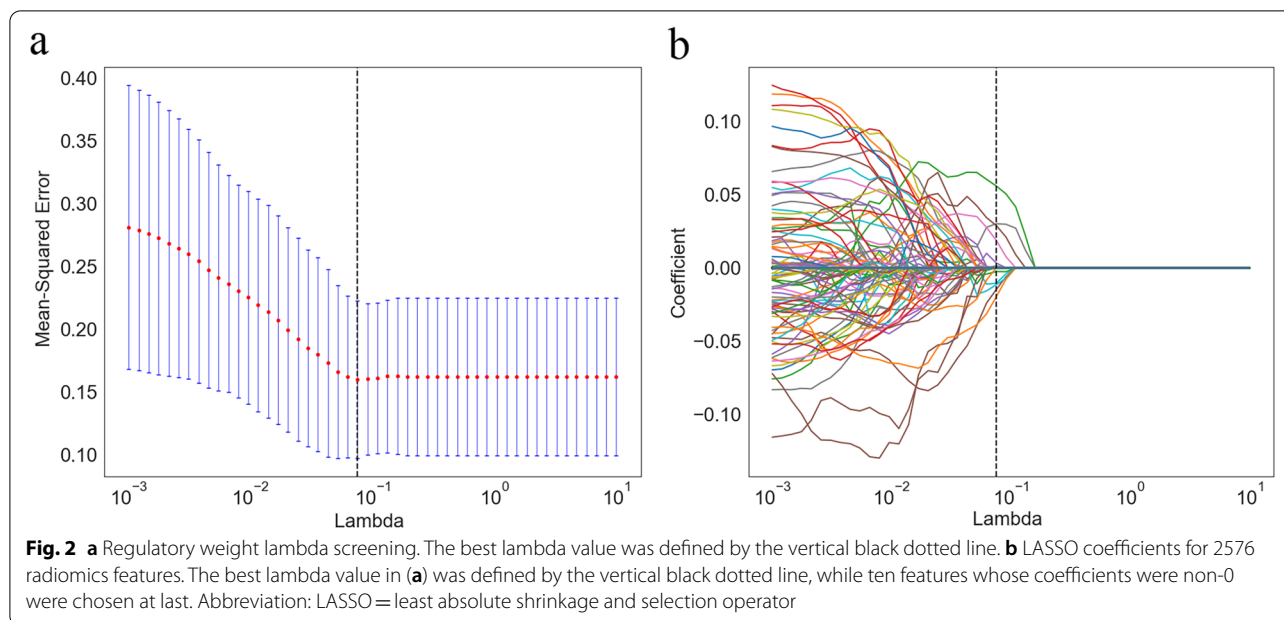


**Table 2** Radiomics feature selection results of lasso regression in Phases II

Structure	Transformation	Type	Feature	Abbreviation
PTV	original	shape	MajorAxisLength	OSMAL_PTV
PTV	original	shape	Sphericity	OSS_PTV
PTV	exponential	glcm	Correlation	EGC_PTV
Lung	original	shape	Maximum2DDiameterRow	OSMax2DDR_Lung
Lung	logarithm	firstorder	Minimum	LFMin_lung
Lung	logarithm	firstorder	TotalEnergy	LFTE_Lung
Lung	exponential	firstorder	Maximum	EFMax_Lung
Lung	exponential	firstorder	MeanAbsoluteDeviation	EFMAD_Lung
Lung	exponential	glszm	SmallAreaLowGrayLevelEmphasis	EGSALG_Lung
Lung	exponential	ngtdm	Contrast	ENC_Lung

(PLT\_3W) of RT was significantly different ( $P = 0.011$ ) between the groups.

**Multivariate analysis of single-phase data and fusion phases data**

The variable correlation coefficient after univariate analysis and feature selection is shown in Fig. 3. The multivariate analysis of single phases and fusion phases is depicted in Table 5. In the phase I model, smoking status is strongly correlated with sex ( $r > 0.8$ ). Since smoking status ( $P = 0.004$ ) was more significant than sex ( $P = 0.01$ ) in the univariate analysis, sex was disregarded. The stepwise logistic regression result illustrated that smoking status was an independent risk factor (odds ratio [OR] = 0.27; 95% confidence interval

[CI]: 0.08–0.85;  $P = 0.025$ ). Similarly, OSMAL\_PTV (OR = 1.02, 95% CI: 1.00–1.03,  $p = 0.018$ ), LFMin\_lung (OR = 1.01, 95%CI: 1.00–1.02,  $P = 0.003$ ), Lungs\_V5 (OR = 1.13, 95% CI: 1.03–1.23,  $P = 0.011$ ), Esophagus\_V10 (OR = 1.05, 95% CI: 1.00–1.11,  $P = 0.025$ ), PLT\_3W (OR = 0.98, 95% CI: 0.97–1,  $P = 0.014$ ) were significant risk factors in Phase II/III/IV model. The independent risk factors of the four single phase models were fused by the RT timeline. Stepwise logistic regression was then performed for Phase I ~ II/I ~ III/I ~ IV models. Notably, the independent risk factors in the Phase I ~ II model comprised only two radiomics features without smoking status (OR = 0.3, 95% CI: 0.09–1.07,  $P = 0.064$ ). Factors independently predicting RP risk in Phase I ~ III model involved clinical, radiomics, and



**Table 3** Univariate regression results for dosimetry parameters in Phases III

Dosimetry parameters	RP < 2 (n = 73)	RP ≥ 2 (n = 18)	p-value
<b>Lung</b>			
V5(%)	48.14 (7.44)	54.58 (6.91)	0.001**
V10(%)	35.93 (5.96)	40.79 (5.25)	0.002**
V15(%)	28.99 (5.31)	32.96 (4.66)	0.004**
V20(%)	23.56 (4.74)	26.25 (3.81)	0.028*
V25(%)	19.38 (4.68)	21.08 (3.69)	0.157
V30(%)	16.07 (4.69)	17.17 (3.79)	0.355
V35(%)	13.19 (4.61)	13.96 (3.75)	0.514
V40(%)	10.69 (4.41)	11.1 (3.56)	0.718
V45(%)	08.47 (4.06)	8.68 (3.18)	0.841
V50(%)	6.43 (3.65)	6.39 (2.79)	0.957
Mean (GY)	12.96 (2.57)	14.21 (1.94)	0.056
<b>Heart</b>			
V10(%)	31.74 (14.98)	36.7 (20.41)	0.246
V20(%)	20.92 (11.12)	22.35 (16.36)	0.661
V30(%)	13.87 (8.58)	12.62 (11.23)	0.605
V40(%)	8.48 (6.28)	6.9 (7.81)	0.365
V50(%)	4.52 (4.1)	3.34 (3.99)	0.126
Mean (GY)	11.23 (5.18)	11.92 (6.62)	0.634
<b>Esophagus</b>			
V10(%)	49.2 (13.29)	60.39 (13.41)	0.002**
V20(%)	41.3 (14.44)	49.81 (16.77)	0.032*
V30(%)	35.09 (15.63)	39.72 (13.17)	0.250
V40(%)	28.42 (16.36)	32.67 (11.35)	0.204
V50(%)	20.84 (15.8)	24.24 (11.83)	0.395
Mean (GY)	21.71 (8.19)	25.23 (6.33)	0.092
<b>SpinalCord</b>			
max (GY)	38.73 (3.90)	38.29 (3.17)	0.277

1. Data are Mean (standard deviation); 2. \*P < 0.05, \*\*P < 0.01; 3. Vx = percentage of structure volume receiving xGy

dosimetry features. As PLT\_3W (OR: 0.99, 95% CI: 0.97–1.00, P = 0.248) was eliminated from the Phase I~IV model, the components of independent factors were consistent with Phase I~III. The discriminatory ability of all model-independent risk factors was analyzed using ROC. The model area under curve (AUC), specificity, and sensitivity can be obtained from Table 6, and ROC visualization and AUC trends from Fig. 4. Notably, the AUC of Phase II (radiomics feature) model is highest in the single phase (AUC: 0.82, 95%CI: 0.70–0.94, Specificity: 0.82, Sensitivity: 0.72), followed by the Phase III (dosimetry parameters) model (AUC: 0.80, 95%CI: 0.67–0.92, Specificity: 0.74, Sensitivity: 0.77). The AUC of the fusion model steadily increased with the radiotherapy timeline, and the results of the ROC analysis for the Phase I~III and Phase I~IV models are observed to be the same.

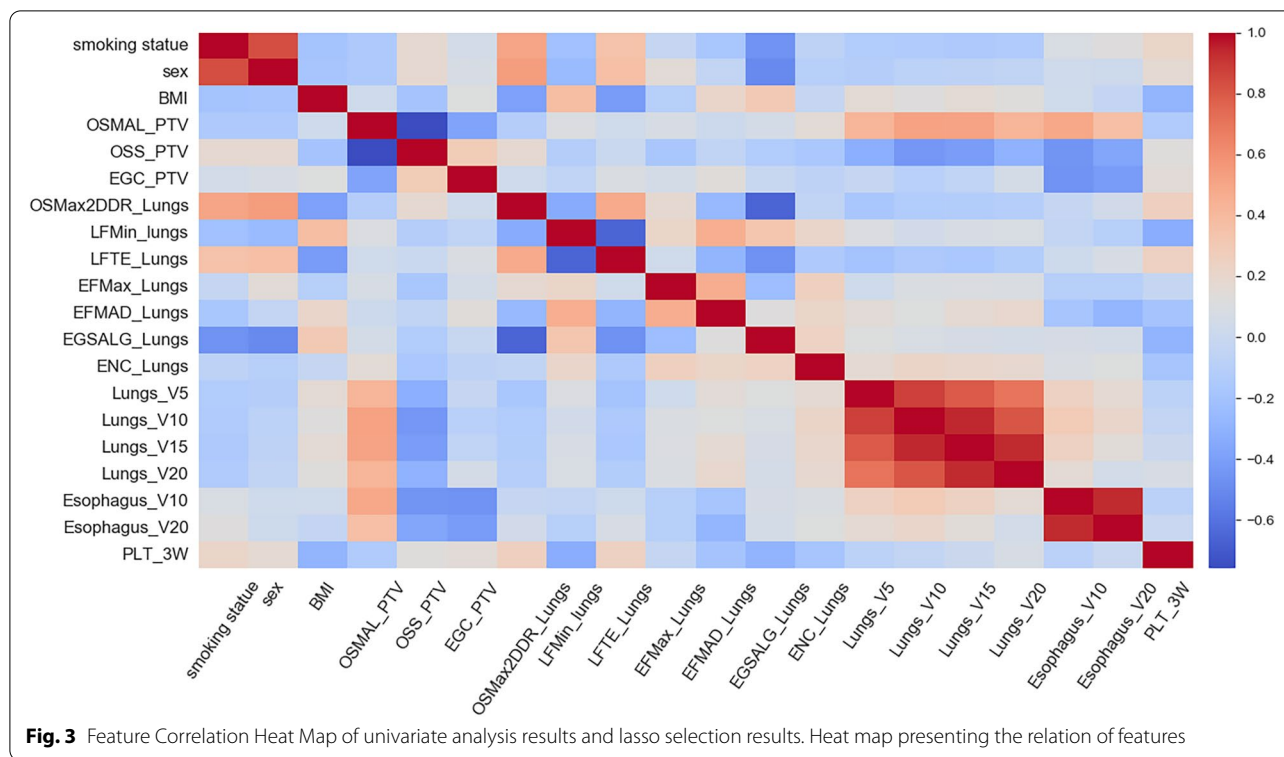
**Table 4** Univariate regression results for Hematological indexes in Phases IV

Hematological indexes	RP < 2 (n = 73)	RP ≥ 2 (n = 18)	p-value
<b>Neutrophils</b>			
baseline (10 <sup>9</sup> /L)	3.94 (2.06)	3.76 (2.69)	0.202
3W (10 <sup>9</sup> /L)	4.05 (4.73)	3.09 (2.01)	0.405
5W (10 <sup>9</sup> /L)	5.23 (5.63)	4.81 (4.24)	0.881
△3W	1.12 (0.99)	1.16 (1.01)	0.738
△5W	2.15 (5.02)	2.01 (2.47)	0.488
<b>Lymphocytes</b>			
baseline (10 <sup>9</sup> /L)	1.79 (0.59)	1.93 (0.84)	0.393
3W (10 <sup>9</sup> /L)	0.78 (0.35)	0.84 (0.41)	0.521
5W (10 <sup>9</sup> /L)	0.57 (0.30)	0.56 (0.23)	0.914
△3W	0.46 (0.19)	0.58 (0.67)	0.701
△5W	0.34 (0.17)	0.38 (0.40)	0.621
<b>Monocytes</b>			
baseline (10 <sup>9</sup> /L)	0.60 (0.32)	0.59 (0.38)	0.902
3W (10 <sup>9</sup> /L)	0.59 (0.35)	0.55 (0.28)	0.612
5W (10 <sup>9</sup> /L)	0.66 (0.38)	0.66 (0.30)	0.679
△3W	1.25 (1.19)	1.77 (2.26)	0.900
△5W	1.88 (4.03)	1.80 (1.49)	0.256
<b>Erythrocytes</b>			
baseline (10 <sup>12</sup> /L)	3.97 (0.63)	3.90 (0.75)	0.686
3W (10 <sup>12</sup> /L)	3.80 (0.55)	3.69 (0.78)	0.463
5W (10 <sup>12</sup> /L)	3.71 (0.66)	3.45 (0.84)	0.157
△3W	0.98 (0.22)	0.94 (0.09)	0.607
△5W	0.95 (0.24)	0.88 (0.15)	0.249
<b>Hemoglobin</b>			
baseline (g/L)	122.98 (15.49)	122.50 (18.19)	0.909
3W (g/L)	117.54 (15.91)	116.61 (19.88)	0.833
5W (g/L)	115.96 (19.99)	112.78 (22.69)	0.557
△3W	0.96 (0.11)	0.95 (0.095)	0.778
△5W	0.95 (0.14)	0.92 (0.14)	0.495
<b>Platelets</b>			
baseline (10 <sup>9</sup> /L)	213.36 (69.17)	209.61 (69.59)	0.837
3W (10 <sup>9</sup> /L)	184.18 (52.25)	148.67 (48.55)	0.011*
5W (10 <sup>9</sup> /L)	185.02 (69.93)	160.50 (88.12)	0.209
△3W	0.91 (0.28)	0.78 (0.34)	0.097
△5W	0.91 (0.32)	0.76 (0.27)	0.079

1. Data are Mean (standard deviation); 2. \*P < 0.05; 3. △3W = the ratio of change at 3 weeks; △5W = the ratio of change at 5 weeks

**Nomogram and risk classification system**

Our nomogram based on Phase I~IV model is presented in Fig. 5. It included variables as follows: smoking status and LFMIn\_lung, lungs\_V5, Esophagus\_V10. The calibration curve verified well calibration of our constructed nomogram (Fig. 6a). DCA suggested that the risk analysis model might have good clinical benefits (Fig. 6b). The risk classification system, based on nomogram score, is shown in Fig. 7. The cases were classified as three



diverse  $RP \geq 2$  risk levels: low-(score 0–135), intermediate-(135–160), or high-risk group ( $> 160$ ), with the prevalence rates being 3.6% (2/55), 30.7% (8/26), and 80.0% (8/10), respectively. In this study, our established risk classification system was precise in differentiating cases having diverse  $RP \geq 2$  risk levels, therefore, facilitating decision-making in the clinic.

**Discussion**

Smoking status was an independent risk factor in Phase I/I~III/I~IV models, which was supposed to be the protective factor for  $RP \geq 2$  ( $OR < 0.3, P < 0.05$ ). In this study, the percentage of smokers or non-smokers with  $RP \geq 2$  was 12.31% (8/65) and 38.46% (10/26), respectively. These data suggested that smokers may be more tolerant to RT than non-smokers, which was in line with the related studies signifying the relation of smoking with a decreased hypersensitivity pneumonitis risk, possibly due to the immunosuppressive effect [24, 25]. However, that does not signify that patients are encouraged to smoke, as smoking affects lung cancer survival [26, 27]. It has been reported that there was no relationship between sex and  $RP \geq 2$  [8, 28]. The risk of  $RP \geq 2$  was 40% (8/20) in female and 14.08% (10/71) in male, depicting a higher risk in female when compared with male. Moreover, the difference was statistically significant ( $P < 0.05$ ) and

possibly associated with a much smaller female lung volume than the male lung volume ( $2055 \pm 457 \text{ cm}^3$  vs.  $3207 \pm 745 \text{ cm}^3, P < 0.001$ ). Under similar dose and radiation field conditions, with the smaller lung volume and the larger the relative volume dose in female. However, sex was strongly correlated with smoking status ( $r > 0.8$ ), with 0% (0/20) of women smoking and 91.5% (65/71) of men smoking. Sex was not involved in the multivariate analysis, therefore, further research was desired to determine the association of sex as an influential factor in  $RP \geq 2$ .

The osmal\_ptv, which was a PTV shape feature extracted from the target area by using the radiomics method, was an independent risk factor ( $or > 1.00, P < 0.05$ ) of Phase II/I~II models that directly reflected the length information of the target area in the principal axis direction. Under similar conditions, the longer the target area, the larger the lung volume involved in RT, and the higher the risk of  $RP \geq 2$ . However, the statistical significance of osmal\_ptv for Phase I~III/I~IV models was not significant ( $P > 0.05$ ), possibly due to the introduction of the dosimetry parameters, particularly esophagus\_V10 parameter. Presently, no literature has reported that esophagus dose was the direct influencing factor of RP. According to the anatomical relationship between the esophagus and lung, we predict that Esophagus\_V10 can indirectly reflect the length

**Table 5** Multivariable analysis results of single Phase and fusion Phase

	Coef	P-value	OR	VIF (max)
Phases I				1.06
Smoking (compared to non-smoking)	-1.2953	0.025*	0.27(0.08-0.85)	
BMI	0.1406	0.168	1.15(0.94-1.40)	
Phases II				1.12
OSMAL_PTV	0.0172	0.018*	1.02(1.00-1.03)	
LFMin_lung	0.0103	0.003**	1.01(1.00-1.02)	
EGC_PTV	-2.5103	0.060	0.08(0.00-1.12)	
Phases III				1.06
Lungs_V5(per 1%)	0.1189	0.011*	1.13(1.03-1.23)	
Esophagus_V10(per 1%)	0.0565	0.025*	1.05(1.00-1.11)	
Phases IV				1.00
PLT_3W	-0.0152	0.014*	0.98(0.97-1)	
Phases I~II				1.08
Smoking (compared to non-smoking)	-1.1966	0.064	0.30(0.09-1.07)	
OSMAL_PTV	0.0195	0.007**	1.02(1.00-1.03)	
LFMin_lung	0.0096	0.007**	1.01(1.00-1.02)	
Phases I~III				1.8
Smoking (compared to non-smoking)	-1.7608	0.021*	0.17(0.04-0.77)	
OSMAL_PTV	0.0031	0.741	1.00(0.98-1.02)	
LFMin_lung	0.0154	0.003**	1.01(1.00-1.02)	
Lungs_V5(per 1%)	0.1163	0.047*	1.12(1.00-1.26)	
Esophagus_V10(per 1%)	0.0977	0.009**	1.10(1.02-1.19)	
Phases I~IV				1.9
Smoking (compared to non-smoking)	-1.7533	0.025*	0.17(0.04-0.79)	
OSMAL_PTV	0.0028	0.769	1.00(0.98-1.02)	
LFMin_lung	0.0142	0.008**	1.01(1.00-1.02)	
Lungs_V5(per 1%)	0.1252	0.042*	1.13(1.00-1.27)	
Esophagus_V10(per 1%)	0.0950	0.010*	1.10(1.02-1.18)	
PLT_3W	-0.0091	0.248	0.99(0.97-1.00)	

1. Data are Mean (standard deviation);2. \*P<0.05, \*\*P<0.01

**Table 6** ROC analysis results of single Phase and fusion Phase

Model	AUC(95% confidence interval)	Sensitivity	Specificity
Phase I	0.67(0.52-0.81)	0.56	0.78
Phase II	0.82(0.70-0.94)	0.72	0.82
Phase III	0.80(0.67-0.92)	0.77	0.74
Phase IV	0.70(0.55-0.84)	0.83	0.60
Phase I~II	0.82(0.70-0.94)	0.72	0.82
Phase I~III	0.90(0.80-1.00)	0.89	0.85
Phase I~IV	0.90(0.80-1.00)	0.89	0.85

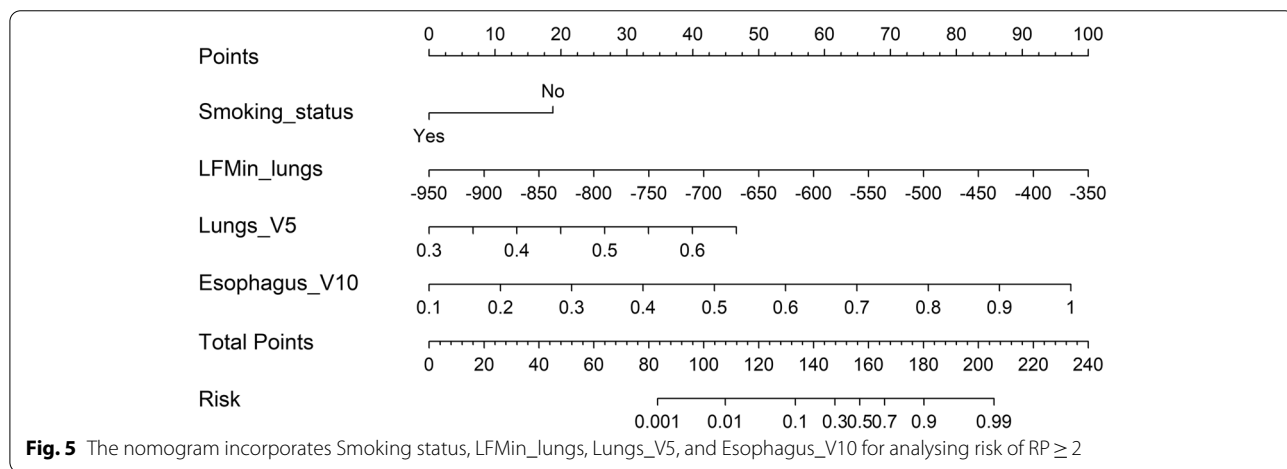
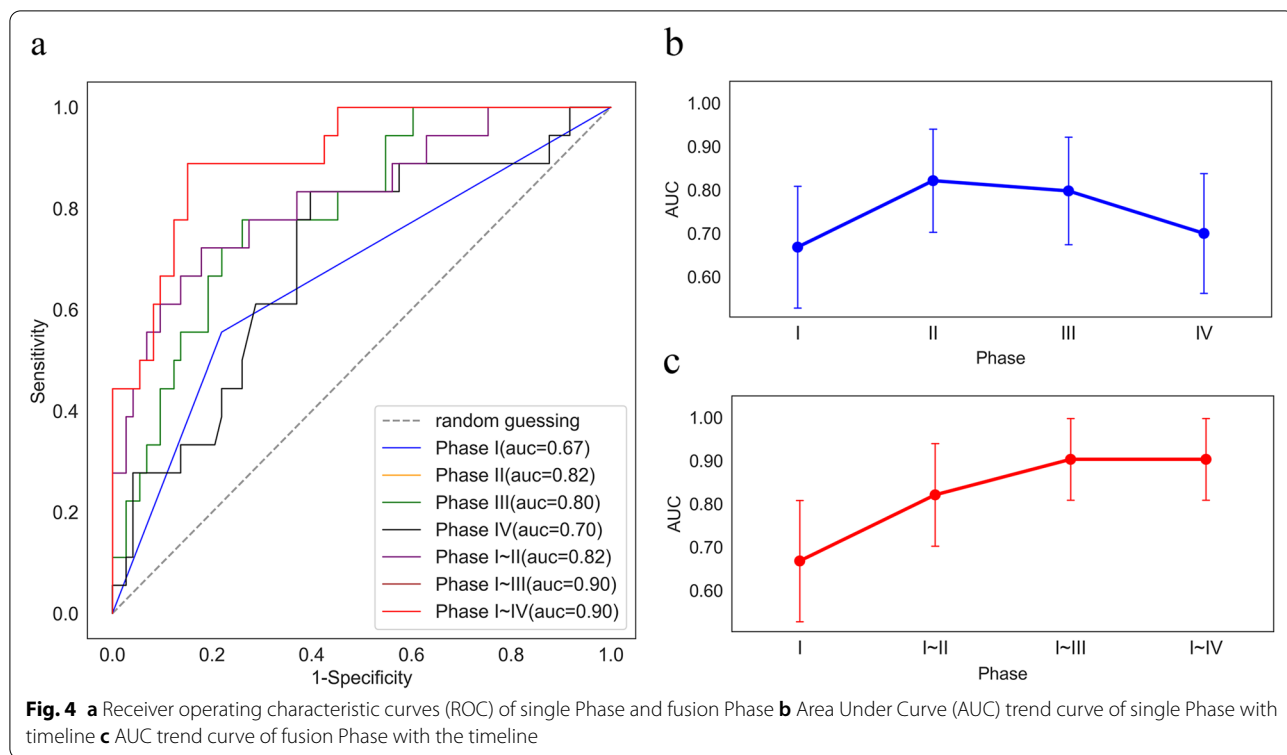
information of the overlapping area of the target area and lung in the transverse position.

In many reports [29-31] that used radiomics to analyze RP risk, rad\_signature was generally constructed based on the linear combination of non-zero coefficient

parameters filtered by lasso regression. In this study, lasso selected ten features, but due to insufficient case data, especially the number of RP-positive patients (18), we avoided using the rad\_signature method but used Spearman's correlation coefficient and stepwise logistic regression to remove variables to avoid overfitting the model with too many variables. Currently, lung tissue radiosensitivity is suggested [32, 33] to be a potential influencing factor for RP. According to our results, LFMin\_lung served as an independent risk factor (or > 1.00, P < 0.05) of Phase II/I ~ II//I ~ III/I ~ IV models. Therefore, we supposed that these radiomics feature extracted from lung CT images might express the RT sensitivity in lung tissues and differentiate susceptible groups with RP ≥ 2 that cannot be obtained from clinical characteristics or dosimetry parameters.

With the free-breathing mode used for the CT scanning modality in this study, it has been suggested that

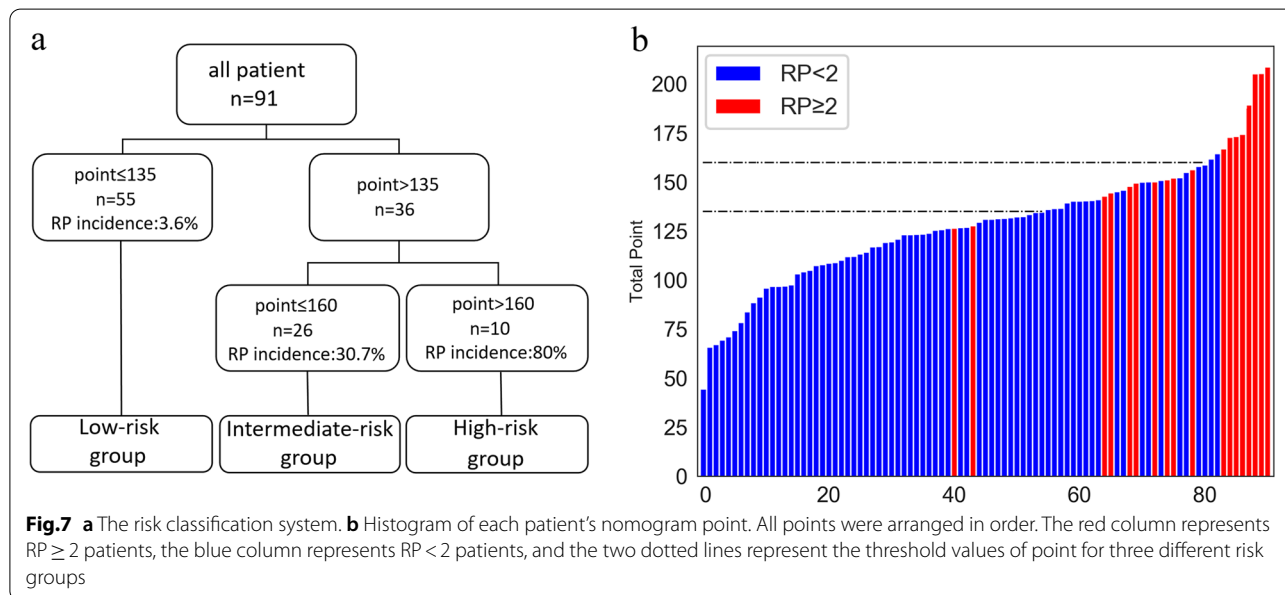
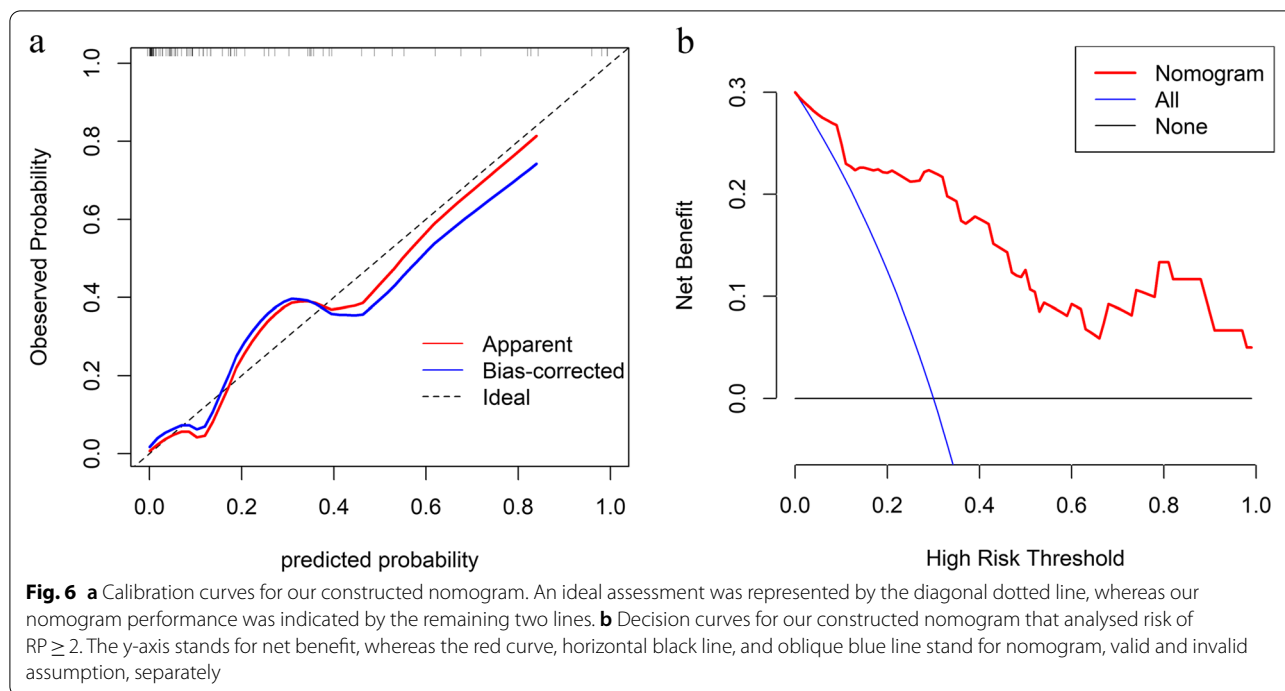




respiratory motion may simply be random noise that influences radiomic features and that features that predict symptomatic RP may be robust and reproducible features of the free-breathing protocol [34]. However, the effect of respiratory motion on radiomic features requires further study. In this paper the ROI of lung was obtained by semi-automatic way segmentation. The steps are as follows: first based on the Eclipse TPS automatic threshold segment tool, then using a manual segmentation method to erase the redundant parts of the lung beyond

the large organs and lung parenchyma for the ROI. Image segmentation is performed by an experienced radiotherapist and then validated by a senior radiotherapist. It has been reported in the literature that manual segmentation is not only time consuming and can cause inter- and intra-observer errors, but semi-automatic segmentation is thought to increase stability [35, 36].

Studies have reported a close relationship between whole lung\_V5 and RP in NSCLC [37–42]. Notably, lung\_V5 was certainly significant for the prediction



of RP among cases having mediastinal lymphoma and esophageal cancer receiving RT [43–45]. Based on the above results, lung\_V5 possibly had a major impact on RP occurrence. As discovered in this work, lung\_V5 was independent risk factor ( $OR > 1, P < 0.05$ ) in Phase III/I~III/1~IV model. We also conducted a univariate ROC analysis on lung\_V5. The best cut-off value was 52.7% (AUC = 0.74, 95%CI: 0.60–0.88, sensitivity = 0.78,

specificity = 0.66). The reason why the cut-off value was only 52.7%, which was less than the dose parameter ( $v5 < 65\%$ ) of guidelines revealed by NCCN to reduce RP risk-limiting lung, might be that our institution has strict restrictions on lung\_V5 in clinical practice ( $v5 < 60\%$ ).

PLT\_3w was considered an independent risk factor ( $OR = 0.98, P = 0.01$ ) in Phase IV model but not in Phase I~IV model ( $OR = 0.99, p = 0.248$ ). However,

it does not signify that platelets are not important because the difference was significant in  $RP \geq 2$  compared with  $RP < 2$  groups upon univariate analysis ( $184.18 \pm 52.25 \times 10^9/L$  vs  $148.67 \pm 48.56 \times 10^9/L$ ,  $P=0.011$ ), with  $PLT\_3W$  being lower in the  $RP \geq 2$  group. Similar results have also been reported in some studies [46] where platelets respond rapidly to resist pathogen invasion. Besides, they have an important effect on adaptive immunomodulation via T cells, B cells, and antigen-presenting cells (APCs). If the platelet number decreases compared to the normal level, patients will have poor immunity and will be more prone to RP. Some inflammatory biomarkers in serum, such as lactate dehydrogenase, C-reactive protein (CRP), tumor necrosis factor (TNF), interleukin, and transforming growth factor (TGF), are related to RP [47, 48]. However, in our study, based on ease of data acquisition, we collected only routine blood count data at different time points during the implementation of radiotherapy. Therefore, we might need further research in this area.

The lung cancer radiotherapy process typically includes admission examination, target area delineation, plan design, and radiotherapy implementation. The time required for the entire process slightly varied from hospital to hospital. For example, it usually took 8–10 weeks in our institution. Thus, we collected data at different phases based on the radiotherapy timeline and conducted a Longitudinal analysis of the risk of  $RP \geq 2$  with RT for NSCLC of stage III/IV. Nevertheless, data regarding this topic remained missing. This work attempted to identify  $RP \geq 2$  risks as early as possible. With the introduction of data at different phases, the AUC values of the model gradually increased, eventually gaining a high AUC value of 0.9 in Phase I~III/I~IV models, higher than any single-phase model. Furthermore, the nomogram and risk classification system established based on the final model are helpful for individualized assessment of  $RP \geq 2$  risk and differentiation of  $RP \geq 2$  population. In the interpretation of our nomogram, we should consider internal validation from the statistical aspect. Apart from ROC survival analysis, this work performed DCA and calibration curves, and these were bootstrap validation approaches. As suggested by clinical statisticians, bootstrap validation is advantageous when the sample size is relatively small [49]. The internal validation results suggested that our nomogram had a satisfactory effect.

This study had several shortcomings, as follows. Firstly, it had a small sample size. More data are necessary for developing and validating our study. Moreover, this was a retrospective study, so there may be selection bias in our data. Third, at present, in our study, only common and important parameters in clinical practice were selected,

including other valuable variables such as genomics and inflammatory markers that may be associated with RP. Therefore, we are also conducting studies in this area.

## Conclusion

In conclusion, the  $RP \geq 2$  risk study based on the radiotherapy timeline found that the  $RP \geq 2$  risk analysis model effect was more accurate as the radiotherapy process had advanced. Finally, we developed a new nomogram and risk classification system by including smoking status, radiomics feature of lungs, and lung and esophageal dose. Our results showed that the model has good performance, which can help doctors recognize high-risk  $RP \geq 2$  NSCLC cases of III/IV stage and guide personalized treatment and clinical decision-making.

## Abbreviations

NSCLC: Non-small-cell lung cancer; RP: Radiation pneumonitis; RT: Radiation therapy; ROI: Region of interest; GTV: Gross tumor volume; CTV: Clinical target volume; PTV: Planning target volume; CSCO: Chinese Society of Clinical Oncology; NCCN: National Comprehensive Cancer Network;  $RP \geq 2$ : Grade  $\geq 2$  Radiation pneumonitis; COPD: Chronic obstructive pulmonary disease; GLCM: Gray Level Concurrence Matrix; GLRLM: Gray Level Run Length Matrix; GLSZM: Gray Level Size Zone Matrix; GLDM: Gray Level Dependence Matrix; NGTDM: Neighbourhood gray-tone difference matrix; LASSO: Least absolute shrinkage and selection operator; ROC: Receiver operating characteristic; DCA: Decision curve analysis;  $PLT\_3W$ : Platelet in the third week; OR: Odds ratio; 95% CI: 95% confidence interval; auc: Area under curve.

## Acknowledgements

We thank the editor and reviewers for relevant and helpful comments on the manuscript.

## Authors' contributions

SHY: conception & design and data collection; SXH: statistical analysis; SHY and SXH: manuscript preparation; XY & KX and BZ: manuscript editing; YRS: quality control of data and manuscript review. All authors read and approved the final manuscript.

## Funding

This work was supported by Hunan Cancer Hospital Climb Plan (KY2021141).

## Availability of data and materials

The full data and materials can be obtained from Shixiong Huang upon sufficient and reasonable request.

## Declarations

### Ethics approval and consent to participate

The study was approved by the Ethics Committee of Hunan Cancer Hospital in accordance with the principles of the Declaration of Helsinki. Approval for a waiver of informed consent for the study was obtained from the Institutional Review Board of Hunan Cancer Hospital. All methods were performed in accordance with the relevant guidelines and regulations.

### Consent for publication

Not applicable.

### Competing interests

The authors declare that they have no competing interests.

### Author details

<sup>1</sup>Department of Clinical Pharmaceutical Research Institution, Hunan Cancer Hospital/the Affiliated Cancer Hospital of Xiangya School of Medicine, Central

South University, Changsha 410013, Hunan, People's Republic of China. <sup>2</sup>Department of Radiation Oncology, Hunan Cancer Hospital/the Affiliated Cancer Hospital of Xiangya School of Medicine, Central South University, Changsha 410013, Hunan, People's Republic of China. <sup>3</sup>Department of Anatomy and Neurobiology, School of Basic Medical Science, Central South University, Morphological Sciences Building, 172 Tongzi Po Road, Changsha 410013, Hunan, China.

Received: 30 July 2022 Accepted: 31 October 2022  
Published online: 07 November 2022

## References

- Lee NS, et al. Predicting 2-year survival in stage I-III non-small cell lung cancer: the development and validation of a scoring system from an Australian cohort. *Radiat Oncol.* 2022;17(1):74.
- Siegel RL, Miller KD, Jemal A. Cancer statistics, 2019. *CA Cancer J Clin.* 2019;69(1):7–34.
- Shi A, et al. Analysis of clinical and dosimetric factors associated with severe acute radiation pneumonitis in patients with locally advanced non-small cell lung cancer treated with concurrent chemotherapy and intensity-modulated radiotherapy. *Radiat Oncol* 2010;5:35.
- Inoue A, et al. Radiation pneumonitis in lung cancer patients: a retrospective study of risk factors and the long-term prognosis. *Int J Radiat Oncol Biol Phys.* 2001;49(3):649–55.
- Semrau S, et al. Concurrent radiochemotherapy with vinorelbine plus cisplatin or carboplatin in patients with locally advanced non-small-cell lung cancer (NSCLC) and an increased risk of treatment complications. Preliminary results. *Strahlenther Onkol.* 2003;179(12):823–31.
- Palma DA, et al. Predicting radiation pneumonitis after chemoradiation therapy for lung cancer: an international individual patient data meta-analysis. *Int J Radiat Oncol Biol Phys.* 2013;85(2):444–50.
- Robnett TJ, et al. Factors predicting severe radiation pneumonitis in patients receiving definitive chemoradiation for lung cancer. *Int J Radiat Oncol Biol Phys.* 2000;48(1):89–94.
- Zhang XJ, et al. Prediction of radiation pneumonitis in lung cancer patients: a systematic review. *J Cancer Res Clin Oncol.* 2012;138(12):2103–16.
- Zhou Z, et al. Pulmonary emphysema is a risk factor for radiation pneumonitis in NSCLC patients with squamous cell carcinoma after thoracic radiation therapy. *Sci Rep.* 2017;7(1):2748.
- Glick D, et al. Impact of pretreatment interstitial lung disease on radiation pneumonitis and survival in patients treated with lung stereotactic body radiation therapy (SBRT). *Clin Lung Cancer.* 2018;19(2):e219–26.
- Li F, et al. Preexisting radiological interstitial lung abnormalities are a risk factor for severe radiation pneumonitis in patients with small-cell lung cancer after thoracic radiation therapy. *Radiat Oncol.* 2018;13(1):82.
- Pan WY, et al. Combining NLR, V20 and mean lung dose to predict radiation induced lung injury in patients with lung cancer treated with intensity modulated radiation therapy and chemotherapy. *Oncotarget.* 2017;8(46):81387–93.
- Ryckman JM, et al. Correlation of dosimetric factors with the development of symptomatic radiation pneumonitis in stereotactic body radiotherapy. *Radiat Oncol.* 2020;15(1):33.
- Nakamura M, et al. Dosimetric factors predicting radiation pneumonitis after CyberKnife stereotactic body radiotherapy for peripheral lung cancer. *Br J Radiol.* 2016;89(1068):20160560.
- Liang B, et al. Dosiomics: extracting 3D spatial features from dose distribution to predict incidence of radiation pneumonitis. *Front Oncol.* 2019;9:269.
- Bashir U, et al. Imaging heterogeneity in lung cancer: techniques, applications, and challenges. *AJR Am J Roentgenol.* 2016;207(3):534–43.
- Yip SS, Aerts HJ. Applications and limitations of radiomics. *Phys Med Biol.* 2016;61(13):R150–66.
- Cunliffe A, et al. Lung texture in serial thoracic computed tomography scans: correlation of radiomics-based features with radiation therapy dose and radiation pneumonitis development. *Int J Radiat Oncol Biol Phys.* 2015;91(5):1048–56.
- Krafft SP, et al. The utility of quantitative CT radiomics features for improved prediction of radiation pneumonitis. *Med Phys.* 2018;45(11):5317–24.
- Lambin P, et al. Radiomics: extracting more information from medical images using advanced feature analysis. *Eur J Cancer.* 2012;48(4):441–6.
- Gillies RJ, Kinahan PE, Hricak H. Radiomics: images are more than pictures, they are data. *Radiology.* 2016;278(2):563–77.
- Fave X, et al. Can radiomics features be reproducibly measured from CBCT images for patients with non-small cell lung cancer? *Med Phys.* 2015;42(12):6784–97.
- Mukaka MM. Statistics corner: a guide to appropriate use of correlation coefficient in medical research. *Malawi Med J.* 2012;24(3):69–71.
- Blanchet MR, Israël-Assayag E, Cormier Y. Inhibitory effect of nicotine on experimental hypersensitivity pneumonitis in vivo and in vitro. *Am J Respir Crit Care Med.* 2004;169(8):903–9.
- Margaritopoulos GA, et al. Smoking and interstitial lung diseases. *Eur Respir Rev.* 2015;24(137):428–35.
- Janjigian YY, et al. Pack-years of cigarette smoking as a prognostic factor in patients with stage IIIB/IV nonsmall cell lung cancer. *Cancer.* 2010;116(3):670–5.
- Shiono S, et al. Smoking is a perioperative risk factor and prognostic factor for lung cancer surgery. *Gen Thorac Cardiovasc Surg.* 2015;63(2):93–8.
- Yamaguchi S, et al. Radiotherapy for thoracic tumors: association between subclinical interstitial lung disease and fatal radiation pneumonitis. *Int J Clin Oncol.* 2015;20(1):45–52.
- Wang L, et al. Computed tomography-based delta-radiomics analysis for discriminating radiation pneumonitis in patients with esophageal cancer after radiation therapy. *Int J Radiat Oncol Biol Phys.* 2021;111(2):443–55.
- Du F, et al. A novel nomogram model based on cone-beam CT radiomics analysis technology for predicting radiation pneumonitis in esophageal cancer patients undergoing radiotherapy. *Front Oncol.* 2020;10:596013.
- Sugai Y, et al. Impact of feature selection methods and subgroup factors on prognostic analysis with CT-based radiomics in non-small cell lung cancer patients. *Radiat Oncol.* 2021;16(1):80.
- Xu L, et al. Genetic variants of SP-D confer susceptibility to radiation pneumonitis in lung cancer patients undergoing thoracic radiation therapy. *Cancer Med.* 2019;8(5):2599–611.
- Yin M, et al. Genetic variants of the nonhomologous end joining gene LIG4 and severe radiation pneumonitis in nonsmall cell lung cancer patients treated with definitive radiotherapy. *Cancer.* 2012;118(2):528–35.
- Jiang W, et al. Dosimetric factors and radiomics features within different regions of interest in planning CT images for improving the prediction of radiation pneumonitis. *Int J Radiat Oncol Biol Phys.* 2021;110(4):1161–70.
- Lu K, Xue Z, Wong ST. A robust semi-automatic approach for ROI segmentation in 3D CT images. *Annu Int Conf IEEE Eng Med Biol Soc.* 2013;2013:5119–22.
- Parmar C, et al. Robust Radiomics feature quantification using semiautomatic volumetric segmentation. *PLoS One.* 2014;9(7):e102107.
- Luna JM, et al. Predicting radiation pneumonitis in locally advanced stage II-III non-small cell lung cancer using machine learning. *Radiother Oncol.* 2019;133:106–12.
- Tang X, et al. Predicting severe acute radiation pneumonitis in patients with non-small cell lung cancer receiving postoperative radiotherapy: development and internal validation of a nomogram based on the clinical and dose-volume histogram parameters. *Radiother Oncol.* 2019;132:197–203.
- Sheng L, et al. Risk factors of grade  $\geq 2$  radiation pneumonitis after gemcitabine induction chemotherapy for patients with non-small cell lung cancer. *Radiat Oncol.* 2019;14(1):229.
- Katsui K, et al. Radiation pneumonitis after definitive concurrent chemoradiotherapy with cisplatin/docetaxel for non-small cell lung cancer: analysis of dose-volume parameters. *Cancer Med.* 2020;9(13):4540–9.
- Watanabe S, et al. Relationship between radiation pneumonitis following definitive radiotherapy for non-small cell lung cancer and Isodose line. *In Vivo.* 2021;35(6):3441–8.
- Yu JH, et al. Study of the predictors for radiation pneumonitis in patient with non-small cell lung cancer received radiotherapy after pneumonectomy. *Cancer Radiother.* 2021;25(4):323–9.
- Cella L, et al. Modeling the risk of radiation-induced lung fibrosis: irradiated heart tissue is as important as irradiated lung. *Radiother Oncol.* 2015;117(1):36–43.

44. Pinnix CC, et al. Predictors of radiation pneumonitis in patients receiving intensity modulated radiation therapy for Hodgkin and non-Hodgkin lymphoma. *Int J Radiat Oncol Biol Phys.* 2015;92(1):175–82.
45. Wang SL, et al. Investigation of clinical and dosimetric factors associated with postoperative pulmonary complications in esophageal cancer patients treated with concurrent chemoradiotherapy followed by surgery. *Int J Radiat Oncol Biol Phys.* 2006;64(3):692–9.
46. Yafeng L, et al. Construction and verification of a radiation pneumonia prediction model based on multiple parameters. *Cancer Control.* 2021;28:10732748211026671.
47. Kong FM, Wang S. Nondosimetric risk factors for radiation-induced lung toxicity. *Semin Radiat Oncol.* 2015;25(2):100–9.
48. Hartsell WF, et al. Can serum markers be used to predict acute and late toxicity in patients with lung cancer? Analysis of RTOG 91-03. *Am J Clin Oncol.* 2007;30(4):368–76.
49. Validation of prediction models, in “Clinical prediction models: a practical approach to development, validation, and updating”. In: Steyerberg EW, editors. Springer: Science+Business Media; 2009. p. 329–44.

### Publisher's Note

Springer Nature remains neutral with regard to jurisdictional claims in published maps and institutional affiliations.

Ready to submit your research? Choose BMC and benefit from:

- fast, convenient online submission
- thorough peer review by experienced researchers in your field
- rapid publication on acceptance
- support for research data, including large and complex data types
- gold Open Access which fosters wider collaboration and increased citations
- maximum visibility for your research: over 100M website views per year

At BMC, research is always in progress.

Learn more [biomedcentral.com/submissions](https://biomedcentral.com/submissions)

